DMD Fast Forward. Published on March 12, 2007 as doi:10.1124/dmd.106.013219

METABOLISM OF PRAZOSIN IN RAT, DOG AND HUMAN LIVER MICROSOMES AND CRYOPRESERVED RAT AND HUMAN HEPATOCYTES AND CHARACTERIZATION OF METABOLITES BY LC/MS/MS

John C. L. Erve*, Sarvesh C. Vashishtha, William DeMaio and Rasmy E. Talaat

Drug Safety and Metabolism

Wyeth Research, 500 Arcola Road, Collegeville, Pennsylvania (J.C.L.E, S.C.V, W.D, R.E.T.)

Running title: IN VITRO METABOLISM OF PRAZOSIN

* Corresponding author: John Erve

Address: Wyeth, 500 Arcola Road, Collegeville, PA, 19426, USA.

Telephone: +484-865-9542; Fax: +484-865-9403; E-mail: ERVEJ@wyeth.com

Number of text pages: 28

Number of tables: 1

Number of figures: 11

References: 32

Number of words in the Abstract: 238

Number of words in the Introduction: 587

Number of words in the Discussion: 1,498

Abbreviations: [1]LC/MS, liquid chromatography/mass spectrometry; DQ, dimethoxy quinazoline-2,4-diamine; GLC, gas-liquid chromatography; GSH, glutathione; ESI, electrospray ionization; HPLC, High-performance liquid chromatography; LC, liquid chromatography; MS, mass spectrometry; MS/MS, tandem mass spectrometry; PTSD, post-traumatic stress disorder; Q-TOF, quadrupole time-of-flight; TOF, time-of-flight; UDPGA, uridine 5'-diphosphoglucuronic acid.

DMD Fast Forward. Published on March 12, 2007 as DOI: 10.1124/dmd.106.013219
This article has not been copyedited and formatted. The final version may differ from this version.

ABSTRACT

Prazosin, (2-[4-(2-furanoyl)-piperazin-1-yl]-4-amino-6,7-dimethoxyquinazoline), is an antihypertensive agent that was introduced to the market in 1976. It has since established an excellent safety record. However, *in vitro* metabolism of prazosin has not been investigated. This study describes the *in vitro* biotransformation of prazosin in liver microsomes from rats, dogs, and humans as well as rat and human cryopreserved hepatocytes and characterization of metabolites using liquid chromatography tandem mass spectrometry. The major *in vivo* biotransformation pathways reported previously in rats and dogs include demethylation, amide hydrolysis and *O*-glucuronidation. These metabolic pathways were also confirmed in our study. In addition, several new metabolites were characterized including a stable carbinolamine, an iminium species and an enamine all formed via oxidation of the piperazine ring. Two ring-opened metabolites generated following oxidative cleavage of the furan ring were also identified. Using semicarbazide hydrochloride as a trapping agent, an intermediate arising from opening of the furan ring was captured as a pyridazine product. In the presence of glutathione, three glutathione conjugates were detected in microsomal incubations, although they were not detected in cryopreserved hepatocytes. These data support ring opening of the furan via a reactive γ-keto-α, β-unsaturated aldehyde intermediate. In the presence of UDPGA, prazosin underwent conjugation to form an *N*-glucuronide not reported previously. Our *in vitro* investigations have revealed additional metabolic transformations of prazosin and have demonstrated the potential of prazosin to undergo bioactivation through metabolism of the furan ring to a reactive intermediate.

INTRODUCTION

Prazosin, 2-[4-(2-furanoyl)-piperazin-1-yl]-4-amino-6,7-dimethoxyquinazoline (Fig. 1), a short acting vasodilator discovered in the mid 1970s, has been widely used in treating hypertension and congestive heart failure (Constantine, 1974; Althius and Hess, 1977; Stanaszek et al., 1983). It was the first of a new class of direct acting vasodilators acting by α-adrenoreceptor blockade. Prazosin was introduced to the United States market as MINIPRESS^{TM} by Pfizer in 1976. Prazosin is well tolerated with the most common side effect associated with treatment being postural hypotension. Although no longer a major drug amongst the anti-hypertensive agents, based on prazosin's ability to antagonize centrally located α_1-adrenergic receptors, a new indication for treatment of post-traumatic stress disorders (PTSD) encountered during civilian life is being explored in clinical studies (Taylor and Raskind, 2002). In addition, prazosin is also being investigated in treating combat-related nightmares characteristic of PTSD among soldiers recently returned from Operation Iraqi Freedom (Daly et. al., 2005).

In vitro metabolism of prazosin in animals or humans has not been reported. Early metabolism studies with ^{14}C-labeled prazosin (label in quinazoline ring) in rats and dogs revealed that it undergoes extensive hepatic metabolism with biliary excretion as the major route of elimination. In the dog, approximately 50% of the drug is metabolized through first pass metabolism. Between 74 and 79% of the intravenous dose was recovered in rat and dog feces, respectively, while urinary excretion was low (Rubin et. al., 1979). In humans, prazosin is highly bound to plasma protein and readily absorbed from the gastrointestinal tract with oral bioavailability ranging from 44 to 77% and a half-life from 2.2 to 3.7 hrs (Bateman et. al., 1979).

In vivo, the primary metabolic route of prazosin consists of 6-*O* and 7-*O*-demethylation followed by glucuronidation (Taylor et al., 1977) with 6-hydroxy-prazosin glucuronide the major metabolite. Other routes of metabolism include hydrolysis of the amide linkage to yield 2-(1-piperazinyl)-4-amino- 6,7-dimethoxyquinazoline (*N*-desfuranoyl prazosin) and to a lesser extent, piperazine ring opening and *N*-dealkylation to give dimethoxy quinazoline-2, 4-diamine (DQ). These metabolites are less potent in lowering blood pressure than prazosin (Althuis and Hess, 1977). The metabolism of prazosin in humans has not been investigated extensively and only *N*-desfuranoyl prazosin has been identified as a metabolite in humans (Piotrovskii et. al., 1984).

Since the initial investigation of prazosin metabolism reported in 1977, there have been tremendous developments in mass spectrometry, most notably, the wide availability of atmospheric pressure ionization techniques such as electrospray and atmospheric chemical ionization. Liquid chromatography/mass spectrometry (LC/MS^1) techniques are now routinely applied in the pharmaceutical industry for metabolite profiling and metabolite identification during drug discovery and development (Nassar et al., 2006). In addition, *in vitro* tools such as liver microsomes, recombinant expressed cytochrome P450 and cryopreserved hepatocytes are readily available facilitating metabolism investigations (Venkatakrishnan, et al., 2001). In the intervening decades since the release of prazosin, interest has increased in the reactive metabolites of various drugs due to their potential to elicit toxicity. Researchers have identified numerous functional groups on drugs that can be bioactivated (Kalgutkar et al., 2005), including unsubstituted furan rings as found on prazosin, and it is not uncommon for pharmaceutical companies to screen for reactive metabolites as part of a comprehensive effort to design safe drugs (Caldwell and Yan, 2006 and the references cited therein). In light of these considerations,

the purpose of the present study was to investigate the *in vitro* metabolism of prazosin, including its bioactivation potential, using rat, dog and human liver microsomes and rat and human cryopreserved hepatocytes combined with state of the art liquid chromatography/ mass spectrometry techniques.

METHODS

Materials. Prazosin hydrochloride, β-nicotinamide adenine dinucleotide phosphate ($NADP^+$), NADPH, glucose 6-phosphate, glucose 6-phosphate dehydrogenase, uridine 5'-diphosphoglucuronic acid (UDPGA) triammonium salt, β-glucuronidase from *E. Coli*, type VII-A (1000 units/vial), glutathione (GSH), semicarbazide hydrochloride and magnesium chloride were all purchased from Sigma Chemical Co. (St. Louis, MO). EDTA (0.5M, pH 8.0) was obtained from GibcoBRL (Grand Island, NY). High-performance liquid chromatography (HPLC) grade acetonitrile and methanol were obtained from EMD Chemicals (Gibbstown, NJ). Formic acid was obtained from Fisher Scientific (Fair Lawn, NJ). All other reagents were of analytical grade.

Pooled liver microsomes from 361 male Sprague-Dawley (SD) rats, four male beagle dogs and pooled mixed gender human liver microsomes from 50 individuals, pooled liver cytosols from 200 male Sprague-Dawley (SD) rats, four male beagle dogs and ten male human liver cytosols were purchased from XenoTech LLC (Lenexa, KS). Pooled rat cryopreserved hepatocytes (Lot # 42514) and human cryopreserved hepatocytes from a female donor (Lot # 30, donor 51) were purchased from BD-Gentest (Woburn, MA). Hepatocyte incubation media, serum free and hepatocyte thawing media were purchased from In Vitro Technologies (Baltimore, MD).

Microsomal Incubation Conditions. Prazosin hydrochloride (10 μM) was incubated in a 1.0 mL solution containing magnesium chloride (10 mM), EDTA (2 mM) in potassium phosphate buffer (0.1 M, pH 7.4), rat, dog or human liver microsomes (1.0 mg/mL), in the presence or absence of an NADPH generating system (2.62 mM of NADP, 7.11 mM of glucose-6-phosphate,

and 0.8 units/mL of glucose-6-phosphate dehydrogenase), and UDPGA, at 37 °C for 2 hr. To assess β-glucuronidase hydrolysis of the aromatic amine *N*-glucuronide, the incubated mixture of prazosin, UDPGA and human liver microsomes in phosphate buffer was incubated with β-glucuronidase (250 units) at pH 5.0 and 7.4 for 24 hr at 37 °C. The incubation mixture without β-glucuronidase was treated as a control. To investigate the stability of metabolites M2, M5 and M8, after performing a human microsomal incubation as described above, an aliquot was evaporated to dryness under N_2, reconstituted in phosphate buffer and incubated at 37 °C for 24 hrs.

Prazosin was also incubated under the conditions mentioned above with rat, dog or human liver cytosol (1 mg/mL) and microsomes (1 mg/mL), GSH (2.5 mM) and an NADPH regenerating system. To trap reactive intermediates of prazosin, semicarbazide hydrochloride (2 mM final concentration) was added to the rat, dog or human liver microsomes incubations together with an NADPH regenerating system. Incubations of prazosin in buffer and in microsomes without NADPH were run as controls.

Studies with Cryopreserved Rat and Human Hepatocytes. The cells were stored in liquid nitrogen until use. Immediately before use, vials of hepatocytes were rapidly thawed in a shaking water bath (37 ^{o}C, 1.5 min) and then immediately transferred to a 50 mL centrifuge tube that had been pre-cooled on ice. Tubes were kept on ice and 24 mL of ice-cold thawing media were added dropwise at a rate of about 4 mL/min with gentle handshaking to prevent the cells from settling. The cell suspension was centrifuged at 50 x g for 5 min at 4 °C, the supernatants

were discarded and the pellets were re-suspended in ice-cold incubation media (6 mL/tube). With gentle handshaking, air was introduced into the suspensions using an automatic pipette until the cells were suspended in the media and the suspensions from the two tubes were pooled. The cell number and viability were determined by the trypan blue exclusion assay (Berry et al., 1969) prior to drug incubations. Prazosin was incubated in 12-well plates at a concentration of 10 μM at 1.0 mL per well containing human hepatocyte suspensions (1.9 million human hepatocytes, viability 37%) or rat hepatocyte suspensions (2.3 million rat hepatocytes, viability 49%) in a gassed (5% CO_2) incubator at 37 °C for 4 hr. Control samples without hepatocytes were also run.

Sample Preparation. At the end of the hepatocyte or microsomal incubations, tubes were transferred to an ice bath. Each sample was extracted with methanol (3 mL), by mixing, sonication and centrifugation at 1,640 × g for 15 min at 4 °C. After each centrifugation, the supernatants were transferred to centrifuge tubes and were evaporated to dryness under nitrogen gas at 20 °C. The dried extracts were reconstituted in 300 μL of methanol/water (6:4, v/v).

Liquid Chromatography/Mass Spectrometry Analysis

An Agilent model 1100 HPLC system including a binary pump and diode array ultraviolet detector (Agilent Technologies, Palo Alto, CA) was coupled to a mass spectrometer described below. The ultraviolet detector was set to monitor λ between190 and 600 nm. Separations were accomplished on a Luna C18(2) column (250 x 2.0 mm, 5 μm) (Phenomenex, Torrance, CA) coupled with a guard cartridge (4 x 2 mm). The sample chamber in the autosampler was maintained at 4 °C, while the column was at ambient temperature of about 22 °C. The mobile

phase consisted of 0.2% formic acid in water (A) and acetonitrile with 0.2% formic acid (B) and was delivered at 0.30 mL/min. The gradient started at 0% B and proceeded linearly to 20% B over 40 minutes, increased to 30% B at 45 minutes, further increased to 45% B at 50 minutes and reached 90% B at 52 minutes before returning to initial conditions at 54 minutes. The total run time was 60 minutes. For hydrogen-deuterium exchange experiments, deuterium oxide was substituted for water in mobile phase A. During LC/MS sample analysis, up to 10 min of the initial flow was diverted away from the mass spectrometer prior to evaluation of metabolites.

Mass spectral data for the metabolites was obtained with a Micromass Q-TOF API-US mass spectrometer (Waters Corp., Milford, MA). It was equipped with an electrospray ionization source and operated in the positive ionization mode. Full scan spectra were acquired from 100 to 1500 *m/z* with a scan time of 0.9 sec. The capillary and cone voltages were 3.5 kV and 25 V, respectively. The source block and desolvation gas temperatures were 120 °C and 350 °C, respectively. The desolvation gas flow was 900 L/hr and the TOF resolution was approximately 8,000 (m/Δm). Argon was used for collision activated dissociation experiments at a pressure setting of 13 psig and the collision offset for acquiring tandem mass spectra varied between 20 – 35 eV depending on the metabolite. The quadrupole radio-frequency setting was 0.2.

RESULTS

Metabolism of Prazosin in NADPH and UDPGA-fortified Liver Microsomes. Incubation of prazosin with liver microsomes fortified with NADPH and UDPGA revealed qualitatively similar metabolite profiles among various species (Fig. 2). Several drug-related components were identified in the microsomal incubation mixture including those that have been identified previously from *in vivo* studies. A number of new metabolites that have not been identified before were also characterized by LC/MS. Following incubation for two hours, prazosin remained the largest component in all species based on UV response (λ = 334 nm). LC/MS analysis indicated the presence of MH^+ ions at *m/z* 290 (M1), 370 (M3, M6), 382 (M5, M8), 384 (prazosin), 400 (M2), 404 (M4), and 418 (M7) (see Table 1).

In human liver microsomal incubations containing both NADPH and UDPGA, LC/MS analysis indicated MH^+ ions at *m/z* 546 (M10, M11) and *m/z* 560 (M13) in addition to those listed above. These three additional metabolites were also observed in rat and dog microsomal incubations and eluted earlier than prazosin, between 25 and 27 minutes (Fig. 2). Although not apparent in Fig 2, when comparing extracted ion chromatograms for *m/z* 546 and *m/z* 560 individually, species differences were evident (data not shown). In particular, for M10, human > rat > dog; M11, rat > human >> dog and M13, human >> rat ~ dog.

Metabolism of Prazosin in NADPH and GSH-fortified Liver Microsomes. In the presence of both NADPH and GSH, LC/MS analysis indicated additional MH^+ ions at *m/z* 709 (M9, M12, M14). These three additional metabolites were observed in rat, dog and human microsomal incubations and eluted earlier than prazosin, between 26 and 28 minutes (data not shown).

Comparing between species, M9 was greatest in humans while M12 was predominant in dogs. In rats, although observed, these metabolites were formed in trace amounts only.

Metabolism of Prazosin in Cryopreserved Rat and Human Hepatocytes. In rat or human cryopreserved hepatocytes, LC/MS analysis revealed many of the same metabolites that were observed in the microsomal incubations with the exception of the GSH conjugates and M11. The profiles produced by rat and human hepatocytes were very similar as seen in Fig. 3. Compared to microsomes, both the oxidative and conjugated metabolites appeared to be less abundant with the exception of M1 and M13, which were the major metabolites in hepatocytes.

Stability of M2, M5 and M8 in buffer. The relative abundance of metabolites M2, M5 and M8 in buffer present at the beginning and end of a 24 hour incubation at T = 37 °C in phosphate buffer, pH 7.4 were compared to investigate the stability of these metabolites. After 24 hours, M2 had decreased only slightly compared to levels initially present. In contrast, M5, which initially was easily detectable, was absent at 24 hours while M8 had more than doubled.

Identification of Prazosin Metabolites. Prazosin had an HPLC retention time of about 40.9 min and showed a protonated molecular ion (MH^+) at *m/z* 384. The proposed fragmentation scheme and product ions of *m/z* 384 for prazosin are shown in Fig. 1. Cleavage of the amide bond generated *m/z* 288, representing the amino-dimethoxy-quinazoline piperazine system and *m/z* 95, the acylium ion representing the 2-furanoyl moiety, respectively. Cleavage of the piperazine ring with charge retention on the amino-dimethoxyquinazoline or furan side of the molecule yielded product ions at *m/z* 247 or 138, respectively. Cleavage of the amino-

dimethoxyquinazoline portion of prazosin generated the product ions at *m/z* 205, 204 and 203 following gain of one or two protons, or, loss of one proton, respectively. LC/MS conducted with D_2O revealed an MD^+ at *m/z* 387 consistent with the two exchangeable amino protons.

M1. The metabolite M1 had a retention time of about 17.7 min on the HPLC system and showed an MH^+ at *m/z* 290, 94 Da less than for prazosin, suggesting it was a hydrolysis product. LC/MS conducted with D_2O produced an MD^+ at *m/z* 294 and indicated three exchangeable protons, one more than prazosin (data not shown). The product ion at *m/z* 247, identical to prazosin, indicated an unchanged amino-dimethoxyquinazoline group and ethylamine of piperazine. However, the acylium ion at *m/z* 95 representing the 2-furanoyl moiety was absent which was consistent with loss of the furanoyl moiety after hydrolysis of the amide bond. Therefore, M1 was tentatively identified as *N*-desfuranoyl prazosin.

M2. Metabolite M2 had a retention time of about 31.4 min on the HPLC system and showed a MH^+ at *m/z* 400, 16 Da larger than for prazosin, indicating it had undergone mono-oxidation. LC/MS conducted with D_2O produced an MD^+ at *m/z* 404 and indicated three exchangeable protons, one more than prazosin, consistent with hydroxylation (data not shown). Product ions at *m/z* 263, 205 and 138 of which only *m/z* 263 was 16 Da higher than the corresponding ion for prazosin at *m/z* 247 indicated hydroxylation had occurred on the piperazine ring. Therefore, M2 was tentatively identified as hydroxy prazosin.

M3 and **M6**. Metabolites M3 and M6 had retention times of about 36.9 and 38.0 min on the HPLC system, respectively, and showed MH^+ 's at *m/z* 370, 14 Da less than prazosin indicating

that demethylation had occurred. LC/MS conducted with D_2O produced an MD^+ at *m/z* 374 and indicated three exchangeable protons, one more than prazosin, consistent with demethylation of a methoxy group to reveal a hydroxy function (data not shown). Mass spectral data for M3 and M6 were identical. Product ions at *m/z* 233 and 190 were 14 Da less than the corresponding ions at *m/z* 247 and 204 for prazosin supporting a single demethylation event on the amino-dimethoxyquinazoline group. Previously it was reported that the major demethylated metabolite *in vivo* was 6-desmethyl prazosin (Taylor et al., 1977) and we observed that the abundance of M3 was larger than M6. Therefore, M3 and M6 were tentatively identified as 6-desmethyl and 7-desmethyl prazosin, respectively.

M4. The metabolite M4 had a retention time of about 37.4 min on the HPLC system and showed an MH^+ at *m/z* 404, 20 Da higher than for prazosin. LC/MS conducted with D_2O produced an MD^+ at *m/z* 408 and indicated three exchangeable protons, one more than prazosin (data not shown). The proposed fragmentation scheme and product ions of *m/z* 404 mass spectrum for M4 are shown in Fig. 4. Loss of 18 Da from MH^+ generated *m/z* 386 indicated the presence of an aliphatic hydroxyl group. The product ion at *m/z* 290, identical to the MH^+ of M1, indicated an unchanged amino-dimethoxyquinazoline piperazine system. No product ion at *m/z* 95 was observed as for prazosin, which indicated metabolism of the furan ring had occurred. Ring opening of furan produced a hydroxybutyryl group ($HO\text{-}CH_2CH_2CH_2\text{-}CO\text{-}$) that generated the product ion at *m/z* 87. In D_2O, the product ion at *m/z* 87 shifted to *m/z* 88. Therefore, M4 was tentatively identified as 5-[4-(4-amino-6,7-dimethoxy-quinazolin-2-yl)-piperazin-1-yl]-4,5-dioxo-pentan-1-ol.

M5. The metabolite M5 had a retention time of about 37.6 min on the HPLC system and showed a protonated MH^+ at *m/z* 382, 2 Da less than prazosin indicating dehydrogenation had occurred. The proposed fragmentation scheme for M5 is shown in Fig. 5. Product ions at *m/z* 245 and 205, of which *m/z* 245 was 2 Da less than the corresponding ion at *m/z* 247 for prazosin, indicated dehydrogenation of the piperazine ring. LC/MS conducted with D_2O revealed an MD^+ at *m/z* 384, which indicated two exchangeable protons, identical to prazosin, and also consistent with a metabolite not requiring protonation for acquiring a charge. Moreover, in D_2O the product ion at *m/z* 245 only shifted 2 Da to *m/z* 247 whereas in prazosin the corresponding ion at *m/z* 247 shifted to *m/z* 250. These observations indicated that M5 possessed a quaternary nitrogen. Two structures in which either one or the other piperazine nitrogen are involved in a carbon-quaternary nitrogen double bond (i.e. iminium ion) following dehydrogenation of the piperazine ring are consistent with this data. Therefore, M5 was tentatively identified as either 4-(4-amino-6,7-dimethoxy-quinazolin-2-yl)-1-(furan-2-carbonyl)-2,3,4,5-tetrahydro-pyrazin-1-ium or 1-(4-amino-6,7-dimethoxy-quinazolin-2-yl)-4-(furan-2-carbonyl)-2,3,4,5-tetrahydro-pyrazin-1-ium.

M7. Metabolite M7 had a retention time of about 39.0 min on the HPLC system and showed a protonated MH^+ at *m/z* 418, 34 Da more than for prazosin. LC/MS conducted with D_2O produced an MD^+ at *m/z* 422 and indicated three exchangeable protons, one more than prazosin (data not shown). The proposed fragmentation scheme and product ions of *m/z* 418 mass spectrum for M7 are shown in Fig. 6. The product ion at *m/z* 290, identical to the MH^+ of M1, indicated an intact amino-dimethoxy-quinazoline piperazine system. No product ion at *m/z* 95 was observed as for prazosin, which indicated metabolism of the furan ring had occurred. Ring opening of furan produced a carboxypropionyl group (HOOC-CH_2CH_2-CO-) that generated the

product ion at *m/z* 101. In D_2O, the product ion at *m/z* 101 shifted to *m/z* 102. Loss of 46 Da (HCOOH) from MH^+ generated *m/z* 372 and supported the presence of a carboxylic acid. Therefore, M7 was tentatively identified as 5-[4-(4-amino-6,7-dimethoxy-quinazolin-2-yl)-piperazin-1-yl]-4,5-dioxo-pentanoic acid.

M8. The metabolite M8 had a retention time of about 44.3 min on the HPLC system and showed a protonated MH^+ at *m/z* 382, 2 Da less than prazosin indicating dehydrogenation had occurred. In H_2O, M8 had an identical spectrum to M5 including observation of product ions at *m/z* 245 and 205, of which *m/z* 245 was 2 Da less than the corresponding ion at *m/z* 247 for prazosin indicating dehydrogenation of the piperazine ring had occurred (see Fig 5 and insert). However, in contrast to M5, LC/MS conducted with D_2O revealed an MD^+ at *m/z* 385 for M8 rather than *m/z* 384 (data not shown). Moreover, in D_2O the product ion at *m/z* 245 shifted 3 Da to *m/z* 248 rather than to *m/z* 247 as observed for M5. These observations support a carbon-carbon double bond (rather than a carbon-quaternary nitrogen double bond) requiring protonation for MS detection. Therefore, M8 was tentatively identified as 2-[4-(2-furanoyl)- 3,4-dihydro-2H-pyrazin-1-yl]-4-amino-6,7-dimethoxyquinazoline.

M10 and **M11**. The metabolites M10 and M11 had retention times of about 31.5 min and 32.7 min on the HPLC system, respectively, and showed a protonated MH^+ at *m/z* 546, 162 Da greater than prazosin indicating they were conjugates. Furthermore, they were both 176 Da larger than the metabolites with *m/z* 370 suggesting that they were glucuronide conjugates of the demethylated metabolites, M3 and M6. Mass spectral data for M10 and M11 were similar. LC/MS conducted with D_2O produced an MD^+ at *m/z* 553 and indicated six exchangeable

protons (data not shown), four more than prazosin and consistent with the introduction of glucuronic acid. The characteristic neutral loss of 176 Da from MH^+ generated the aglycone at *m/z* 370 further supporting the presence of a glucuronide. As described above, M3 was the major *O*-demethylated metabolite. Since M10 was more abundant than M11, M10 and M11 were tentatively identified as glucuronides of 6-*O*-desmethyl and 7-*O*-desmethyl prazosin, respectively.

M13. Metabolite M13 had a retention time of about 33.2 min on the HPLC system and showed a protonated MH^+ at *m/z* 560, 176 Da more than for prazosin indicating it was a conjugate. The characteristic neutral loss of 176 Da from *m/z* 560 generated the aglycone at *m/z* 384 indicating a glucuronide. LC/MS conducted with D_2O produced an MD^+ at *m/z* 566 and indicated five exchangeable protons (data not shown), three more than prazosin and consistent with the introduction of glucuronic acid on the amino group. The quinazoline amino group was the only possible site on unchanged prazosin capable of undergoing conjugation. Therefore, M13 was identified as prazosin *N*-glucuronide.

M9, M12 and **M14**. Metabolites M9, M12 and M14 had retention times of about 30.8, 33.4 and 34.7 min, respectively, on the HPLC system and showed protonated MH^+ at *m/z* 709, which was 325 Da more than for prazosin, indicating they were conjugates. These metabolites were also 305 Da higher than M4 suggesting that M9, M12 and M14 were GSH conjugates derived from M4. LC/MS conducted with D_2O produced an MD^+ at *m/z* 719 and indicated nine exchangeable protons (data not shown) seven more than prazosin and consistent with the introduction of GSH. The proposed fragmentation scheme and product ions of M9 mass spectrum (similar to spectra

for M12 and M14, not shown) are shown in Fig 7. Loss of 129 Da (pyroglutamic acid moiety) from MH^+ with subsequent loss of H_2O generated *m/z* 562 supporting the presence of GSH. The product ion at *m/z* 290, identical to the MH^+ of M1, indicated an intact amino-dimethoxy-quinazoline piperazine system. No product ion at *m/z* 95 was observed as for prazosin which indicated furan had undergone metabolism. The product ion at *m/z* 418 was a result of addition of GSH to the carbonyl hydroxybutyryl group ($HO\text{-}CH_2CH_2CH_2\text{-}CO\text{-}CO$) formed following oxidative cleavage of furan. Therefore, M9, M12 and M14 were tentatively proposed to be GSH conjugates.

Trapping reactive intermediate of Prazosin. In order to further investigate the metabolism of the furan ring of prazosin to a reactive metabolite, M15, incubations were conducted in the presence of 2 mM semicarbazide hydrochloride. The semicarbazide trapped product of M15 had a retention time of about 32.4 min on the HPLC system (Fig 8) and showed a protonated MH^+ at *m/z* 396, 12 Da higher than for prazosin. LC/MS conducted with D_2O produced an MD^+ at *m/z* 399 and indicated two exchangeable protons (data not shown), identical to prazosin. The proposed fragmentation scheme and product ions of the semicarbazide-trapped product of M15 mass spectrum are shown in Fig. 9. The product ion at *m/z* 290, identical to the MH^+ of M1, indicated an unchanged amino-dimethoxyquinazoline piperazine system. No product ion at *m/z* 95 was observed as for prazosin, which indicated furan had undergone metabolism. The observation of an ion at *m/z* 107 was consistent with a pyrazidine acylium ion. Therefore, the semicarbazide-trapped product of M15 was tentatively identified as (1-[4-amino-6,7-dimethoxy-2-quinazoline]-4[2-pyrazidine]-piperazine.

DMD Fast Forward. Published on March 12, 2007 as DOI: 10.1124/dmd.106.013219
This article has not been copyedited and formatted. The final version may differ from this version.

DISCUSSION

One objective of this work was to use current *in vitro* methodology and analytical tools to study the metabolism of prazosin and to determine the correlation with *in vivo* data (Taylor et al., 1977; Piotovskii et al., 1984). Further understanding prazosin metabolism remains relevant due to renewed interest in prazosin for PTSD. In contrast to the first investigations (Taylor et al., 1977) which used a combination of thin layer chromatography and GLC or solid probe mass spectrometric techniques, we used LC/MS for characterization of metabolites. Microsomes and hepatocytes are now routinely used to investigate metabolism of new chemical entities and are important tools in lead optimization of drug candidates (Ekins et al, 2000). In our studies, the major metabolites detected in rats and dogs were also generated *in vitro* and characterized by LC/MS/MS. Microsomes and hepatocytes formed 6-*O* and 7-*O* desmethyl prazosin (M3 and M6) in the expected relative abundance as observed *in vivo* i.e. 6-*O* > 7-*O* desmethyl prazosin. The *in vivo* metabolite *N*-desfuranoyl prazosin (M1) is expected to result from amidase activity. We identified M1 in microsomes and hepatocytes although it was more abundant in hepatocytes. Conversion of M1 to DQ was reported to occur in rats and dogs (Taylor et. al., 1977). Although we observed DQ in microsomal incubations, as its formation was not NADPH dependent and it was also seen in our prazosin stock, it was not deemed a metabolite in our studies. In addition, several new metabolites formed by oxidation of the piperazine ring (M2, M5, and M8), furan cleavage (M4 and M7), GSH conjugation (M9, M12 and M14) and *N*-glucuronidation (M13) were also characterized. These proposed metabolic pathways are shown in Fig. 10 and Fig. 11.

In the presence of UDPGA, microsomes produced two *O*-glucuronides, M10 and M11, derived from M3 and M6, respectively, although in hepatocytes only M10 was detected. *O*-

glucuronides had been proposed to form *in vivo* based on experiments in which Glusulase™ treatment of urine generated aglycones identical to synthetic 6-O and 7-O desmethyl-prazosin (Taylor et al., 1977). In humans these glucuronides have not been reported. In addition to *O*-glucuronides, we also obtained direct evidence for prazosin *N*-glucuronide (M13) in microsomal incubations supplemented with UDPGA. M13 was not detected in previous animal studies perhaps due to its instability under the extraction and isolation conditions employed. Indirect evidence for an *N*-glucuronide of doxazosin, a close structural analog of prazosin, was obtained based on its colorimetric reaction with napthoresorcinol and its resistance to β-glucuronidase activity (Kaye et al., 1986). In mouse it was a major metabolite constituting approximately 17% of the dose, although it was not detected in humans (Kaye et al., 1986). In our studies, M13 was formed in greater amounts than either M10 or M11. With respect to the glucuronide metabolites (M10, M11 and M13), humans showed better concordance with dogs than with rats.

Hydroxylation on the piperazine ring formed M2, a carbinolamine. Carbinolamines are well-recognized metabolic products although acyclic tertiary amines are often unstable and are converted to the corresponding aldehyde (or ketone) and *N*-dealkylated amine (Rose and Castagnoli, 1983). However, for cyclic tertiary amines the carbinolamine is reported to remain in equilibrium with the iminium species (Sayre et al. 1997). Our stability results suggest that M2 is stable based on its continued detection for at least 24 hours. We cannot assign which carbon of the piperazine group is hydroxylated by the product ion spectrum. However, Prakash and Soliman characterized two carbinolamines of a drug candidate formed in rat and argued that delocalization of the nitrogen lone pair electrons, made possible by a pyrimidine or succinimide substituent, imparted stability to these carbinolamines (Prakash and Soliman, 1997). For M2,

these considerations could justify hydroxylation on any of the piperazine carbons as each nitrogen substituent (quinazoline or carbonyl) could allow electron delocalization, although the carbon closest to the carbonyl group might be more likely as it is expected to have greater positive character due to the electronegativity of oxygen. M2 is expected to be in equilibrium with the iminium species, M5, yet with time M5 is converted to the more stable enamine, M8. Uncertainty as to the site of hydroxylation for M2 discussed above, prevents knowing which of two possible iminium structures for M5 exist (see Fig. 5) and a definitive structure awaits isolation and NMR characterization (in progress).

Evidence for furan bioactivation to a reactive γ-keto-α,β-unsaturated aldehyde, M15, included (1) detection of ring-opened metabolites (M4 and M7) (2) trapping M15 with semicarbazide, and (3) detection of GSH conjugates. The proposed pathway leading to these products are shown in Fig. 11. Kobayashi and coworkers reported that metabolism of TA-1801 converted furan first to a hydroxybutyryl group and then to a carboxypropionic acid (Kobayashi et al., 1987a). To explain these ring-opened metabolites, they proposed that furan was metabolized by P450 directly to a γ-keto-α,β-unsaturated aldehyde (Kobayashi et al., 1987b) although an epoxide, as suggested by Le Fur based on studies with diclofurime, (Le Fur and Labaune, 1985) may also generate the γ-keto-α,β-unsaturated aldehyde. M4 and M7 are also hydroxybutyryl and carboxypropionic acid containing metabolites, respectively, and are consistent with Kobayashi's observations. Semicarbazide has been used to trap an unsaturated γ-keto-α,β-unsaturated aldehyde derived from pulegone (McClanahan et al., 1989) as a pyridazine product and we also successfully trapped the γ-keto-α,β-unsaturated aldehyde (M15)

derived from prazosin with semicarbazide. Finally, semicarbazide greatly reduced the formation of M4 and M7 (Fig. 8) consistent with their formation via M15.

Generation of M4 and M7, the former requiring a net 4-electron reduction, may be rationalized based on consideration of possible enzymes involved in their formation via M15. Many reactive γ-keto-α,β-unsaturated aldehydes are toxic and the body has several enzymes to detoxify them. Metabolism of the aldehyde to an alcohol (e.g. carbonyl reductase), oxidation to an acid (e.g. aldehyde dehydrogenase or alcohol dehydrogenase) or conjugation with GSH represent detoxification events (Dick et al., 2001). Double bond reduction by hepatic NAD(P)H oxidoreductase also abolishes reactivity of α,β-unsaturated carbonyls (Dick et al., 2001). Carbon-carbon double bond reductive metabolism has been reported for drugs containing this α,β-unsaturated carbonyl structure (Lindstrom and Whitaker, 1984; Taskinen et al., 1991) and it is possible that NAD(P)H oxidoreductase is also involved in the metabolism of prazosin.

M15 has several sites capable of reacting with GSH. 1,4-Addition of GSH across the double bond with reduction of the aldehyde could produce two distinct GSH conjugates. 1,2-addition of GSH to the aldehyde with reduction of the double bond would generate a GSH conjugate with identical mass. These GSH conjugates, especially that formed through reaction with the aldehyde, may be reversible, although their low abundance precluded a kinetic investigation. It is tempting to assign the three GSH conjugates observed in our incubations to the three possibilities described above. However, we cannot exclude the possibility that two HPLC-peaks represent diastereomers. Therefore, until isolated GSH conjugates are further characterized by NMR it is unwise to speculate on the exact structure of these conjugates. In

our cryopreserved hepatocyte experiments, although furan ring opening was evident based on the presence of M4 and M7, no GSH conjugates were observed. This observation may reflect decreased GSH concentrations as a result of the cryopreservation process, which can be less than 10% of fresh hepatocytes (Sohlenius-Sterbeck and Schmidt, 2005).

Whether our *in vitro* findings of new metabolites of prazosin correlate with *in vivo* metabolism of prazosin will require further studies (in progress). Instrumentation available today can enable detection of even minor metabolites *in vivo*. From a toxicology perspective, however, furan bioactivation may be irrelevant since the toxicity profile of prazosin is established. The primary adverse reaction is postural hypotension and syncope, especially upon initiation of medication, a result of its pharmacological activity (Hoffman and Lefkowitz, 1990). No reports of idiosyncratic toxicity to prazosin are in the literature. Idiosyncratic drug toxicity is often explained by electrophilic reactive intermediates that covalently modify protein and initiate a damaging immune response (Uetrecht, 2003). The risk of causing idiosyncratic drug toxicity is often a justification for implementing screening strategies for reactive metabolites (Caldwell and Yan, 2006). We did not determine if covalent binding to protein occurred and, if so, what levels were reached. Thus, we cannot speculate whether prazosin would have this liability based on guidelines used by some firms (Evans and Baillie, 2005). Kalgutkar has demonstrated with loperamide that although bioactivation to a potentially neurotoxic pyridinium metabolite was detected *in vitro*, the absence of such toxicity in humans when taken as prescribed may reflect mitigating events such as p-glycoprotein activity preventing brain accumulation (Kalgutkar and Ngyuen, 2005). Our work with prazosin provides another reminder that toxicity is often multi-factorial and bioactivation does not always lead to toxicity.

Furthermore, Uetrecht has observed that idiosyncratic toxicity is seldom associated with drugs given at doses of 10 mg or less (Uetrecht, 2001). The absence of idiosyncratic toxicity associated with prazosin, administered at a maximal daily dose of 5 mg for hypertension (Hoffman and Lefkowitz, 1990), or a mean dose of 9.5 mg/day for PTSD (Raskind et al. 2003) supports this empirical observation.

Acknowledgements.

The authors would like to thank Dr. Appavu Chandrasekaran and Dr. JoAnn Scatina for helpful comments and a critical review of the manuscript.

References

Althuis TH and Hess HJ (1977) Synthesis and identification of the major metabolites of prazosin formed in dog and rat. *J Med Chem* 20:146-149.

Bateman DN, Hobbs DC, Twomey TM, Stevens EA, and Rawlins MD (1979) Prazosin, pharmacokinetics and concentration effects. *Eur J Pharmacol* 16:177-181.

Berry MN, Friend DS (1969) High-yield preparation of isolated rat liver parenchymal cells: a biochemical and fine structural study. *J Cell Biol* 43:506–520.

Caldwell GW and Yan Z (2006) Screening for reactive intermediates and toxicity assessment in drug discovery. *Curr Opin Drug Disc Dev* 9:47-60.

Constantine JW (1974) Analysis of the hypotensive action of prazosin, in *Prazosin-Evaluation of a new antihypertensive agent*, (Cotton ed), pp 16-36 Excerpta Medica, Geneva.

Daly CM, Doyle ME, Radkind M, Raskind E, and Daniels C (2005) Clinical case series: the use of Prazosin for combat-related recurrent nightmares among operation Iraqi Freedom combat veterans. *Mil Med* 170:513-515.

Dick RA, Kwak MK, Sutter TR, Kensler TW. (2001) Antioxidative function and substrate specificity of NAD(P)H-dependent alkenal/one oxidoreductase. A new role for leukotriene B4 12-hydroxydehydrogenase/15-oxoprostaglandin 13-reductase. *J Biol Chem*. 276:40803-10.

Ekins S, Ring BJ, Grace J, McRobie-Belle DJ, Wrighton, SA (2000) Present and future *in vitro* approaches for drug metabolism. *J Pharmacol Toxicol Methods* 44: *313-324.*

Evans DC and Baillie TA (2005) Minimizing the potential for metabolic activation as an integral part of drug design. *Current Opinion in Drug Disc & Dev* 8:44-50.

Hoffman, BB and Lefkowitz, RJ (1990) Adrendergic receptor antagonists in *Goodman and Gilman's The pharmacological basis of therapeutics*, (A. Goodman Gilman, ed), pp 221-243, Pergamon Press, 8th Edition, Elmsford, NY.

Kalgutkar AS, Gardner I, Obach RS, Shaffer CL, Callegari E, Henne KR, Mutlib AE, Dalvie DK, Lee JS, Nakai Y, O'Donnell JP, Boer J and Harriman SP (2005) A comprehensive listing of bioactivation pathways of organic functional groups. *Curr Drug Metab* 3:161-225.

Kalgutkar AS, Nguyen HT (2005) Identification of an *N*-methyl-4-phenylpyridinium-like metabolite of the antidiarrheal agent loperamide in human liver microsomes: underlying reason(s) for the lack of neurotoxicity despite the bioactivation event. *Drug Metab Dipos* 9:943-952.

Kaye B, Cussans NJ, Faulkner JK, Stopher DA and Reid JL (1986) The metabolism and kinetics of doxazosin in man, mouse, rat and dog. *Br J Clin Pharmacol* 21 Suppl 1:19S-25S.

Kobayashi T, Ando H, Sugihara, J and Harigaya S (1987a) Metabolism of ethyl 2-(4-chlorophenyl)-5-(2-furyl)-oxazole-4-acetate, a new hypolipidemic agent, in the rat, rabbit and dog. Glucuronidation of carboxyl group and cleavage of furan ring. *Pharmacol Exp Therap* 15:262-266.

Kobayashi T, Sugihara J and Harigaya S (1987b) Mechanism of metabolic cleavage of a furan ring. *Drug Metab Dispos* 15:877-881.

Le Fur JM and Labaune JP (1985) Metabolic pathway by cleavage of a furan ring. *Xenobiotica* 15:567-577.

Lindstrom TD and Whitaker GW. (1984) Saturation of an alpha, beta-unsaturated ketone: a novel xenobiotic biotransformation in mammals. *Xenobiotica*. 14:503-8.

McClanahan RH, Thomassen D, Slattery JT, Nelson SD. (1989) Metabolic activation of (R)-(+)-pulegone to a reactive enonal that covalently binds to mouse liver proteins. *Chem Res Toxicol* 2:349-55.

Nassar AE, Talaat RE, Kamel AM (2006) The impact of recent innovations in the use of liquid chromatography-mass spectrometry in support of drug metabolism studies: are we all the way there yet? *Curr Opin Drug Disc Dev* 9:61-74.

Prakash C and Soliman V (1997) Metabolism and excretion of a novel antianxiety drug candidate, CP-93,393, in Long Evans rats. Differentiation of regioisomeric glucuronides by LC/MS/MS. *Drug Metab Dispos* 25:1288-97.

Piotrovskii VK, Veiko NN, Ryabokon OS, Postolnikov SF and Metelitsa VI (1984) Identification of a prazosin metabolite and some preliminary data on its kinetics in hypertensive patients. *Eur J Clin Pharmacol* 27:275-280.

Raskind MA, Peskind ER, Kanter ED, Petrie EC, Radant A, Thompson CE, Dobie DJ, Hoff D., Rein RJ, Straits-Tröster K, Thomas RG and McFall MM (2003) Reduction of nightmares and other PTSD symptoms in combat veterans by prazosin: A placebo-controlled study. *Am. J. Psychiatry* 160:371-373.

Rose, J, and Castagnoli, N (1983). The metabolism of tertiary amines. *Med Res Rev* 3:73-88

Rubin P, Yee YG, Anderson M and Blaschke T (1979) Prazosin first-pass metabolism and hepatic extraction in the dog. *J Cardiovasc Pharmacol* 1:641-647.

Sayre LM, Engelhart DA, Nadkarni DV, Babu MKM, Flammang AM and McCoy GD (1997) The role of imimium-enamine species in the toxication and detoxication of cyclic tertiary amines in *Pharmacokinetics, metabolism and pharmaceutics of drugs of abuse*, (RS Rapaka, ed), pp 106-127, NIDA, Rockville, MD.

Sohlenius-Sternbeck AK and Schmidt S (2005) Impaired glutathione-conjugating capacity by cryopreserved human and rat hepatocytes. *Xenobiotica* 35:727-736.

Stanaszek WF, Kellerman D, Brogden RN and Romankiewicz JA (1983) Prazosin update. A review of its pharmacological properties and therapeutic use in hypertension and congestive heart failure. *Drugs* 25:339-384.

Taskinen J, Wikberg T, Ottoila P, Kanner L, Lotta T, Pippuri A, Backstrom R. (1991) Identification of major metabolites of the catechol-O-methyltransferase-inhibitor nitecapone in human urine. *Drug Metab Dispos.* 19:178-83.

Taylor LA, Twomey TM and Schuch von Wintenau M (1977) The metabolic fate of prazosin. *Xenobiotica* 7:357-364.

Taylor F and Raskind MA (2002) The α_1-adrenergic antagonist prazosin improves sleep

and nightmares in civilian trauma posttraumatic stress disorder. *J Clin Psychopharmacol* 22:82-85.

Uetrecht, J. (2003) Screening for the potential of a drug candidate to cause idiosyncratic drug reactions. *Drug Discov Today* 15:832-37.

Uetrecht, J. (2001) Prediction of a new drug's potential to cause idiosyncratic reactions. *Curr Opin Drug Discov Dev* 4:55-59.

Venkatakrishnan K, Von Moltke LL, Greenblatt DJ. (2001) Human drug metabolism and the cytochromes P450: application and relevance of *in vitro* models. *J Clin Pharmacol* 41:1149-79.

Figure Legends

Fig. 1. Product ions of *m/z* 384 mass spectrum of prazosin and the proposed origin of key product ions. Insert displays the numbering of the quinazoline ring.

Fig. 2. Extracted ion chromatograms for prazosin and metabolites including the glucuronides produced in microsomal incubations from human (A), rat (B) and dog (C).

Fig. 3. Extracted ion chromatogram for prazosin and metabolites including the glucuronides produced in cyropreserved hepatocytes from human (A), rat (B).

Fig. 4. Product ions of *m/z* 404 mass spectrum of M4 and the proposed origin of key product ions.

Fig. 5. Product ions of *m/z* 382 mass spectrum of M5 (mass spectrum of M8 identical), and the proposed origin of key product ions. For M5, it is unknown which piperazine nitrogen is quaternary. The insert depicts one of two possibilities for the piperazine ring of M5 and the dehydro-piperazine in M8.

Fig. 6. Product ions of *m/z* 418 mass spectrum of M7 and the proposed origin of key product ions.

Fig. 7. Product ions of *m/z* 709 mass spectrum of M9 and the proposed origin of key product ions.

Fig. 8. Extracted ions for M3, M4, M7 and *m/z* 396 (pyridazine product) in the absence (A) or presence (B) of 2 mM semicarbazide.

Fig 9. Product ions of *m/z* 396 mass spectrum of the semicarbazide trapped product of M15, and the proposed origin of key product ions.

Fig. 10. Proposed in vitro metabolism of prazosin. Bold indicates metabolites not previously reported. DQ was not detected *in vitro* but was reported *in vivo*. Only one possible structure for M5 is shown. See Discussion.

Fig. 11. Proposed pathway (via route A or B) for cytochrome P450 mediated ring opening of the furan ring of prazosin to M15 and subsequent formation of GSH conjugates and semicarbazide-trapped product.

DMD Fast Forward. Published on March 12, 2007 as DOI: 10.1124/dmd.106.013219
This article has not been copyedited and formatted. The final version may differ from this version.

TABLE 1

Retention times and mass spectral properties for prazosin and its metabolites observed in vitro

Metabolite	Rt (min)	MH^+	MD^+	*m/z* of select product ions
Prazosin	40.9	384	387	288, 247, 231, 204, 164, 138, 120, 95
M1	17.7	290	294	247, 231, 221, 203
M2	31.4	400	404	382, 287, 263, 245, 205, 138, 95
M3	36.9	370	374	352, 233, 218, 190, 164, 138, 120, 95
M4	37.4	404	408	386, 370, 290, 247, 221, 205, 140, 87
M5	37.6	382	384	287, 271, 245, 229, 205, 95
M6	38.0	370	374	352, 233, 218, 190, 164, 138, 120, 95
M7	39.0	418	422	402, 290, 247, 231, 205, 126, 101
M8	44.3	382	385	287, 271, 245, 229, 205, 95
M9	30.8	709	719	691, 562, 436, 418, 386, 290, 247
M10	31.5	546	553	370, 352, 233, 138
M11	32.7	546	553	370, 352, 233, 138
M12	33.4	709	719	691, 562, 436, 418, 386, 290, 247
M13	33.2	560	566	456, 426, 384, 247, 233, 138, 95
M14	34.7	709	719	691, 562, 436, 418, 386, 290, 247
M15*	32.4	396	399	290, 247, 231, 203, 176, 150, 107

* Trapped as a pyridazine product

DMD Fast Forward. Published on March 12, 2007 as DOI: 10.1124/dmd.106.013219
This article has not been copyedited and formatted. The final version may differ from this version.

Figure 1

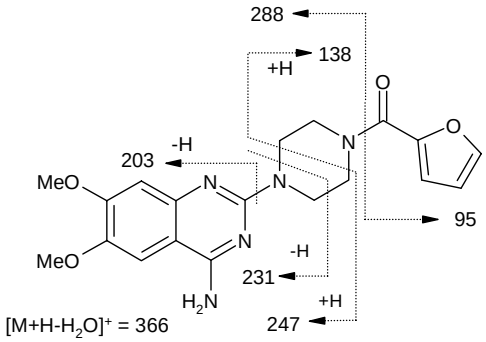

Insert

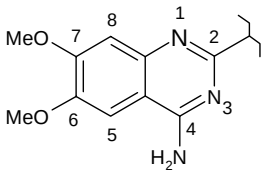

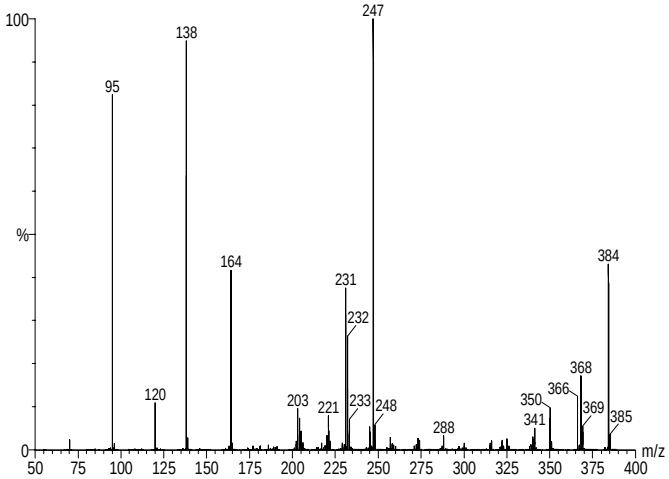

DMD Fast Forward. Published on March 12, 2007 as DOI: 10.1124/dmd.106.013219
This article has not been copyedited and formatted. The final version may differ from this version.

Figure 2

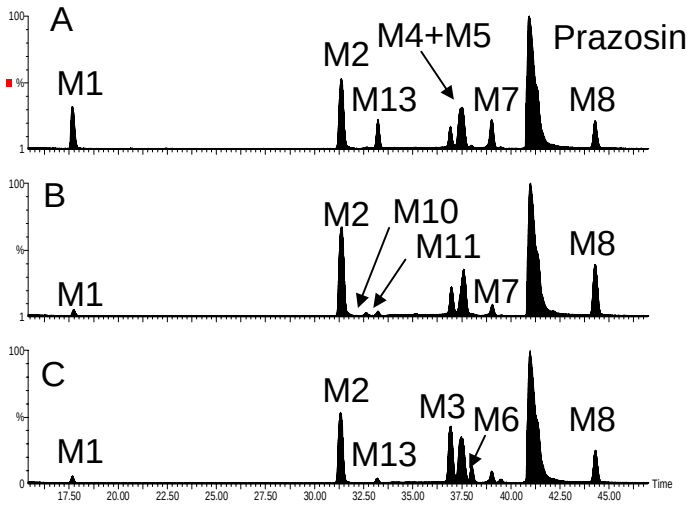

DMD Fast Forward. Published on March 12, 2007 as DOI: 10.1124/dmd.106.013219
This article has not been copyedited and formatted. The final version may differ from this version.

Fig 3

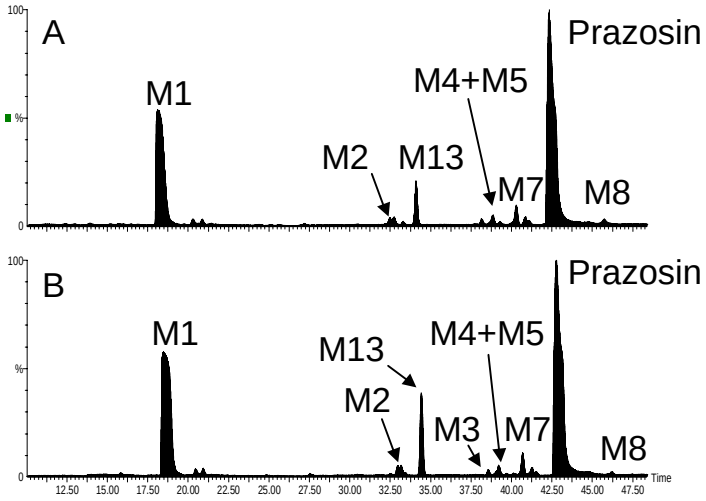

DMD Fast Forward. Published on March 12, 2007 as DOI: 10.1124/dmd.106.013219
This article has not been copyedited and formatted. The final version may differ from this version.

Figure 4

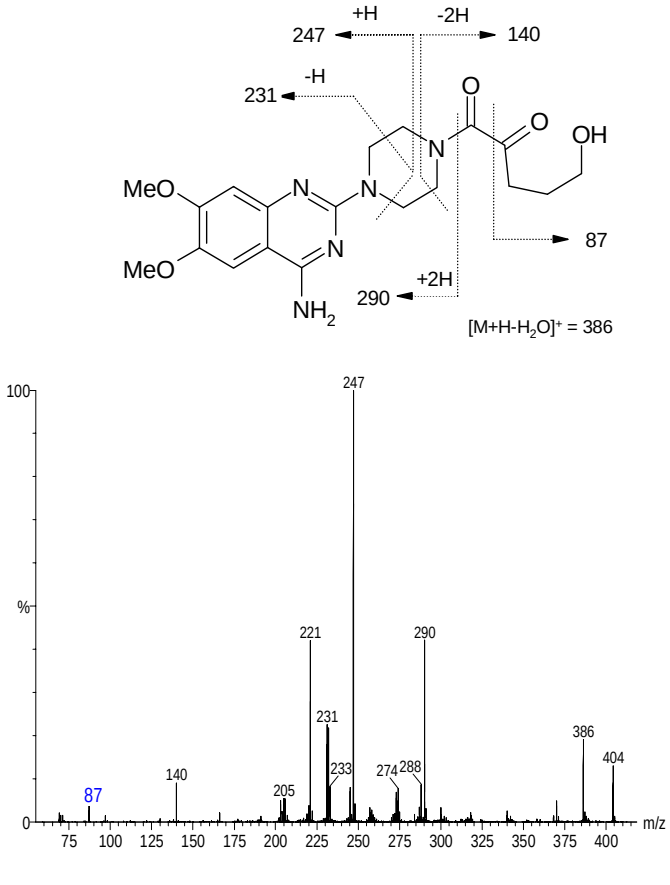

DMD Fast Forward. Published on March 12, 2007 as DOI: 10.1124/dmd.106.013219
This article has not been copyedited and formatted. The final version may differ from this version.

Figure 5

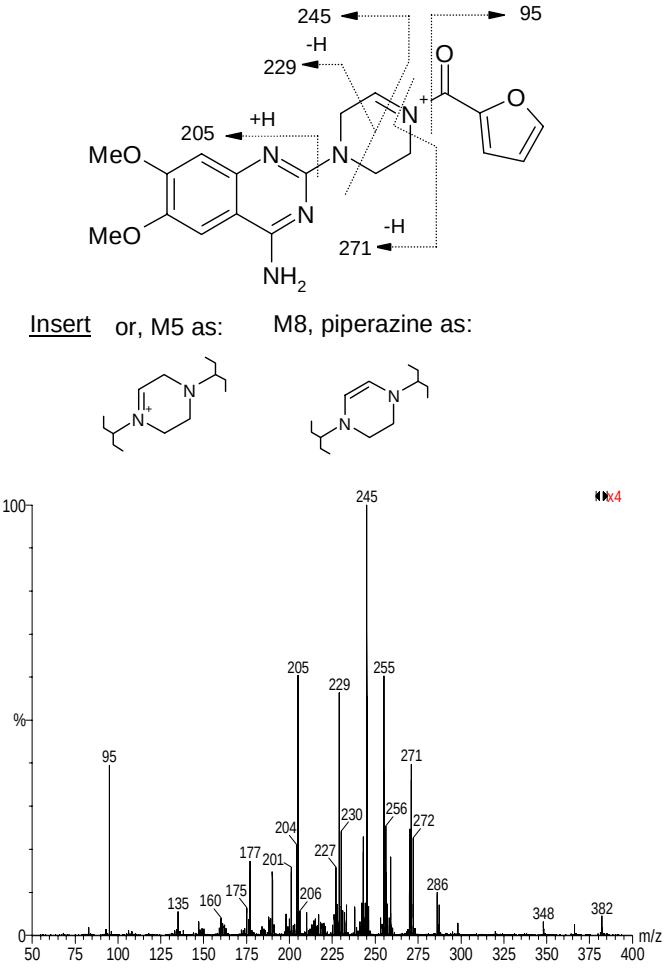

DMD Fast Forward. Published on March 12, 2007 as DOI: 10.1124/dmd.106.013219
This article has not been copyedited and formatted. The final version may differ from this version.

Figure 6

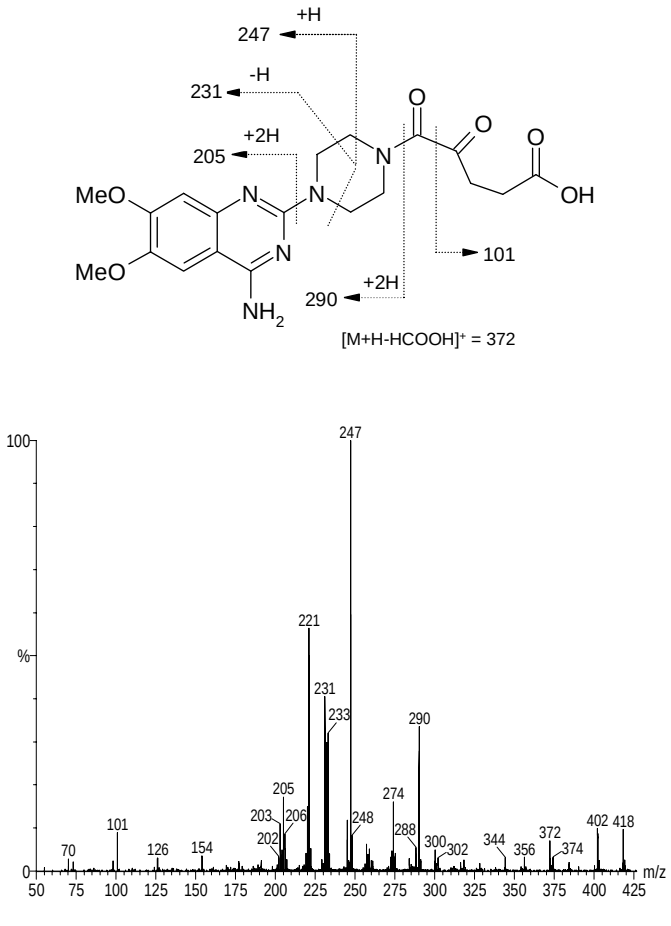

DMD Fast Forward. Published on March 12, 2007 as DOI: 10.1124/dmd.106.013219
This article has not been copyedited and formatted. The final version may differ from this version.

Figure 7

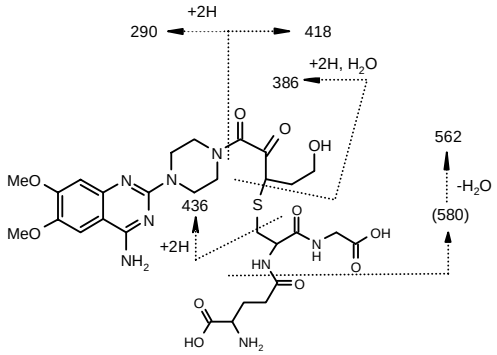

$[M+H-H_2O]^+ = 691$

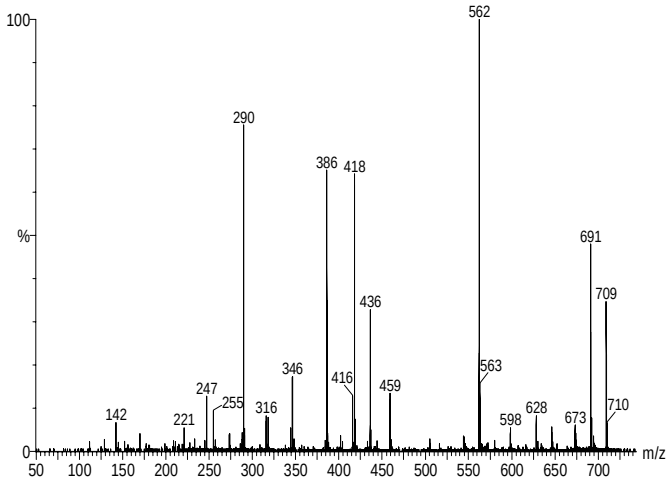

DMD Fast Forward. Published on March 12, 2007 as DOI: 10.1124/dmd.106.013219

Figure 8

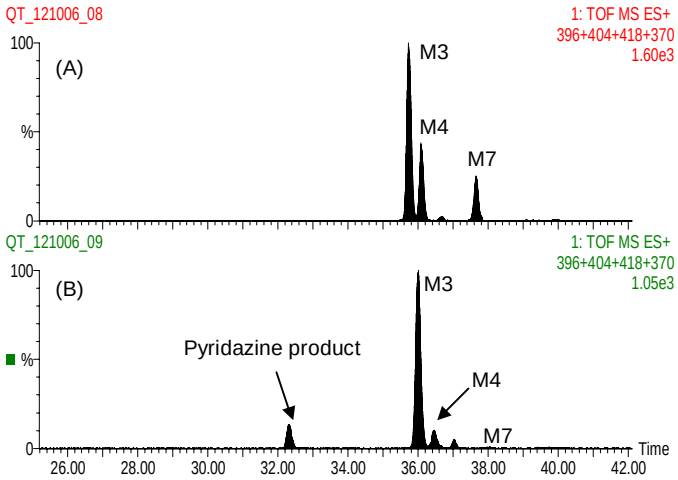

DMD Fast Forward. Published on March 12, 2007 as DOI: 10.1124/dmd.106.013219
This article has not been copyedited and formatted. The final version may differ from this version.

Figure 9

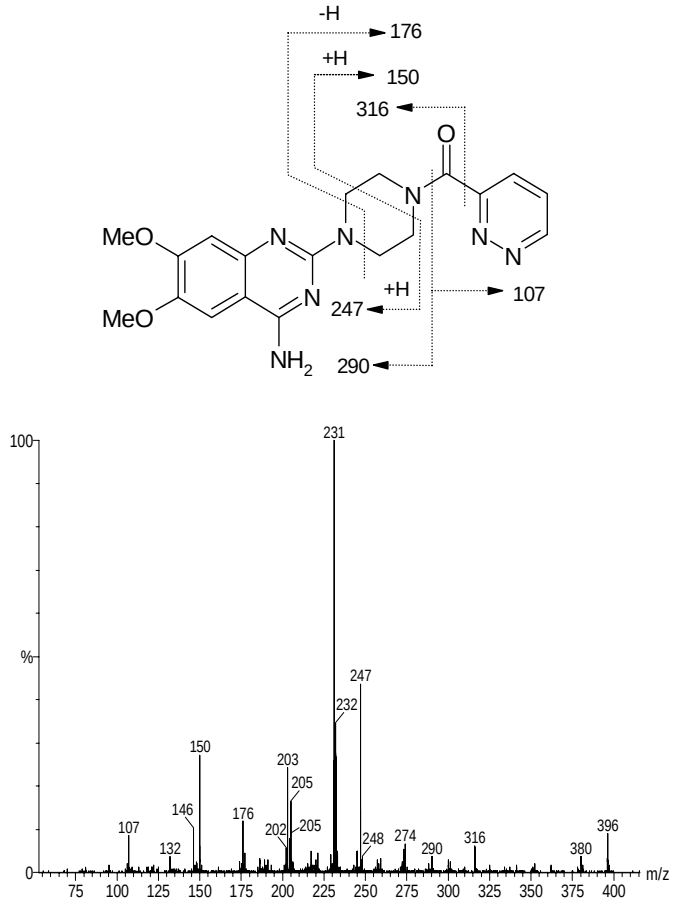

Fig 10

DMD Fast Forward. Published on March 12, 2007 as DOI: 10.1124/dmd.106.013219

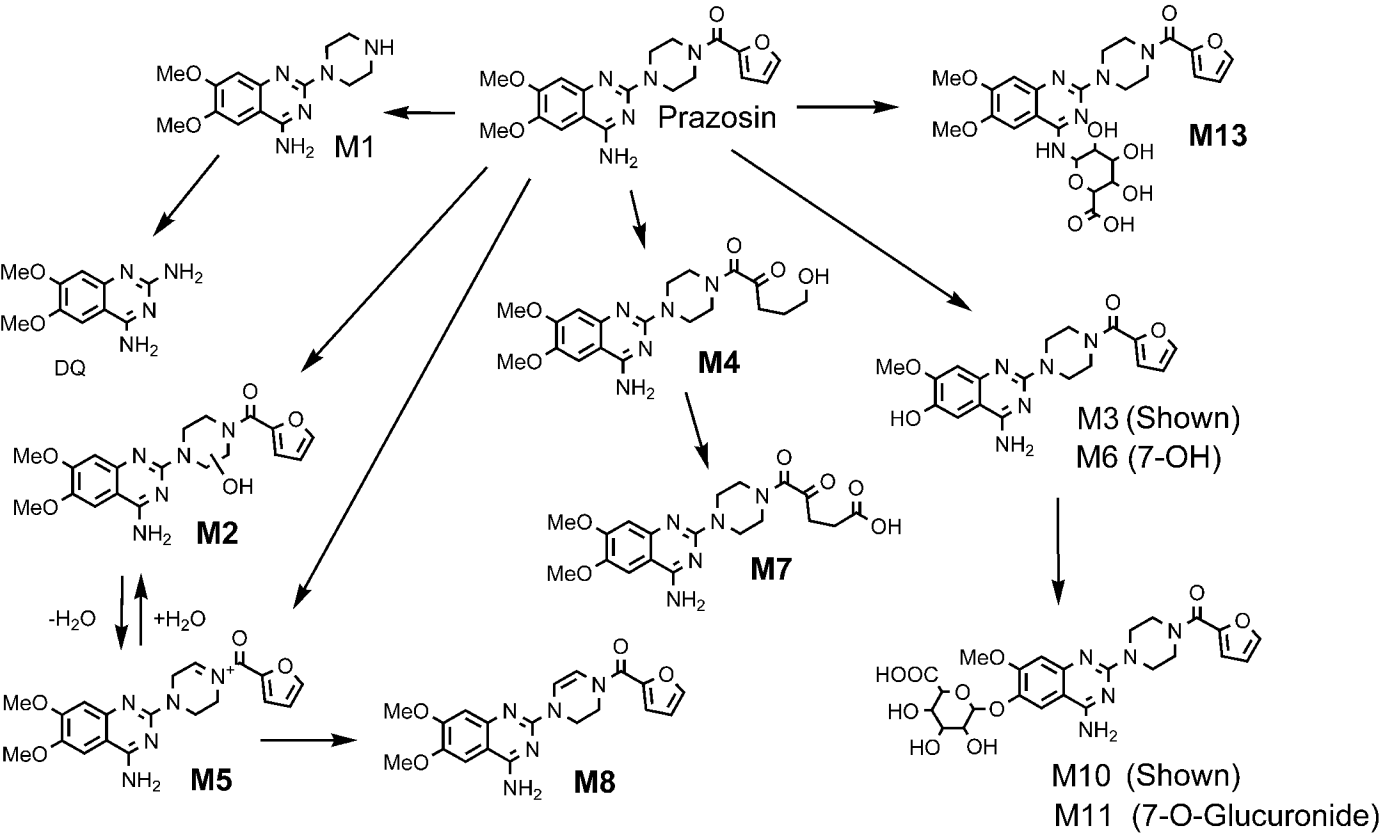

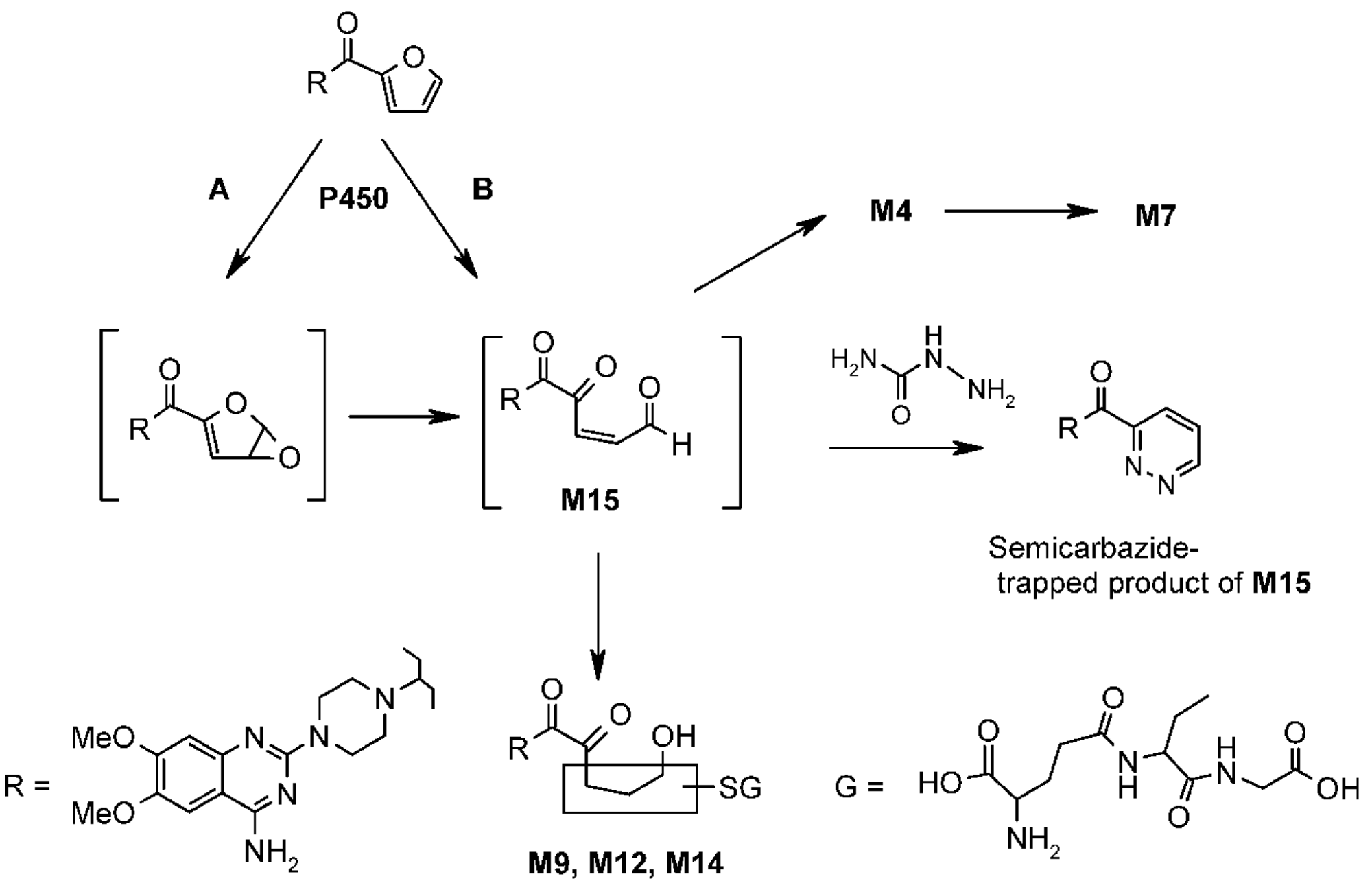
A
P450
B
M4
M7
M15
Semicarbazide-
trapped product of M15
R =
MeO
MeO
NH2
SG
M9, M12, M14
G =
HO
NH2
OH

Fig. 11.